



C

EGYPTIAN ACADEMIC JOURNAL OF

BIOLOGICAL SCIENCES

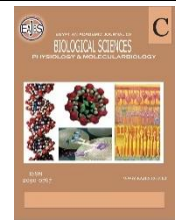
PHYSIOLOGY & MOLECULAR BIOLOGY



ISSN
2090-0767

WWW.EAJBS.EG.NET

Vol. 14 No. 2 (2022)



Effects of the Co-Administration of Thyme and Tramadol on The Postnatal Development of Purkinje Neurons of The Albino Rat

Mohamed El-Badry Mohamed, Hoda Ahmed Mohamed, Ghada Rady Ghait and Mohamed Hashem Mohamed*

Department of Human Anatomy and Embryology, Faculty of Medicine, Assiut University, Egypt.

*E. Mail: dmohamedahmed111@gmail.com

ARTICLE INFO

Article History

Received:3/8/2022

Accepted:27/9/2022

Available:30/9/2022

Keywords:

Postnatal; Purkinje Neurons; Tramadol; Thyme.

ABSTRACT

Background: Tramadol is a painkiller that works by acting on the central nervous system. Even though tramadol is regarded to have minimal misuse and dependence potential, it is increasingly being used in pregnant women in many countries throughout the world, notably in the Middle East, Africa, and West Asia, to relieve pain from rheumatoid arthritis, cancer, and other diseases. **Aim of the work:** To assess the harmful effects of tramadol on the postnatal development of the cerebellar Purkinje cells of rats and to evaluate the possible ameliorative effect of thyme if being administered with tramadol simultaneously. **Material & Methods:** Three sets of Forty-eight mature female albino rats were randomly organized into three equal groups; Group 1 (control), group 2 (tramadol treated) and group 3 (tramadol+thyme treated). The rats' offspring of the fore mentioned three groups were further subdivided according to their ages into 3 subgroups (newborn, 10th, and 20th postnatal day). Group I have not received any treatment. Tramadol HCL (40 mg/Kg/day) dissolved in tab water was given orally to group B. Tramadol (40 mg/Kg/day) and thyme extract (500 mg/kg/day) were given orally to group C. From the first day of pregnancy until weaning, female rats were administered tramadol and thyme. For each of the three groups, the Purkinje cell layer of the cerebellar cortex of the rats' offspring (newborn, 10th, and 20th postnatal day) was then examined for histological, ultrastructural, immunohistochemical changes and morphometric analysis. **Results:** Histological, ultrastructural and immunohistochemistry studies showed that in GII there were neuronal frittering and apoptotic changes in the Purkinje neurons. In GIII, an improvement in histological, ultrastructural and immunohistochemical changes was observed. The morphometric results revealed that there was a significant statistical difference at 10th and 20th postnatal age whereas no recorded significant statistical difference at newborn age among the experimental groups. **Conclusion:** Tramadol use during pregnancy and breastfeeding had a neurotoxic impact on the development of Purkinje cells of the cerebellar cortex of rats. Thyme extract can ameliorate the tramadol's harmful effects; hence it may be useful in the therapy of tramadol neuronal damage if tramadol is required.

INTRODUCTION

In order to treat moderate to severe pain, a prescription for tramadol is valuable. In addition to post-operative pain, cancer pain, and musculoskeletal pain, it is used to treat many other types of pain. As being a centrally acting opioid analgesic, it has a mild inhibition of norepinephrine and serotonin reuptake. So, tramadol is a common pain reliever (Subedi *et al.*, 2019, Dean and Kane, 2021).

Male and female youth with a history of drug misuse and anxiety are increasingly abusing tramadol. Tramadol is used to replace heroin by many adolescent addicts (Ray, Arya and Gupta, 2022, Cicero *et al.*, 2005). Nausea, vomiting, sweating, itching, and constipation are among the most often reported side effects of this medicine. Provoked seizures are most linked to this condition. Physical dependency and withdrawal syndrome have been linked to long-term usage of high dosages of tramadol. Tramadol induces both normal and unusual opiate withdrawal symptoms, such as seizures (Kabel and van Puijenbroek, 2005, Jerjir *et al.*, 2022). Animal studies have indicated that this medication has a bad impact on organ development, bone growth, and mortality rate at extremely high dosages (Boonyarattanasoonthorn, and Kijtaowornrat, 2021).

Normally, tramadol should be avoided during pregnancy since it might produce reversible withdrawal symptoms in the newborn. Tramadol use during pregnancy reduces neuronal survival, synapse formation, and neuronal development in the offspring's cerebrum and cerebellum (Farhan and Mubarak, 2017). Tramadol causes oxidative stress in the progeny cerebellum. This was demonstrated by an increase in lipid peroxidation and a reduction in the antioxidant enzymes' activity (Aboulhoda and Hassan, 2018).

Tramadol inhibits the antioxidant enzymes in the mitochondria of cerebellar neurons, resulting in the production of reactive oxygen species that cause cell injury

(Mohammadnejad and Soltaninejad, 2022, Mohamed *et al.*, 2015).

The cerebellum has the greatest amounts of nitric oxide (NO). NO is a neurotransmitter implicated in brain ageing (Blanco *et al.*, 2010). Tramadol administration results in increased expression of the inducible nitric oxide synthetase (iNOS) and increased synthesis of NO, which has a valuable role in neurotransmission and vasodilation at low doses but is neurotoxic at higher doses (Khatmi *et al.*, 2022, El-Bermawy and Salem, 2015).

Purkinje neurons (PN) are unique cells with remarkable branched dendrites. This allows integrating large amounts of information and learning by remodeling their dendrites. PN is necessary for well-coordinated movement and other areas of function such as cognition and emotion (Paul and Limaieem, 2021). PN affections result in ataxia, neurodegeneration, and altered cerebellar output (Feng *et al.*, 2022).

Thyme is a natural plant of the Mediterranean region, belonging to the Lamiacea family. Thyme is currently widely used as a spice, a tea, and a medicinal herb (El-Newary *et al.*, 2017). The herb thyme contains high amounts of vitamins and minerals. Thymol has been shown in studies to enhance healthy fats and increases omega-3 content in the cell membranes of kidney, heart, and brain cells. Its contents of vitamins, and minerals, as well as rosmarinic and ursolic acids, may help to prevent cancer (Kuate, 2017).

Thymus vulgaris possess various beneficial effects, like antiseptic, antibactericidal, antihelminthic, and antioxidant properties. Also, it has lately been recommended as a natural replacement for synthetic antioxidants. It can trap free radicals, which is an important antioxidant mechanism for inhibiting lipid peroxidation, which is the primary cause of oxidative stress. On the brain tissues, the concurrent use of thyme extract and tramadol improves oxidative stress (Sarhan and Taalab, 2018). Thyme has been shown to have a

neuroprotective effect against brain damage caused by cerebral ischemia-reperfusion via reducing oxidative stress (Setorki and Mirzapoor, 2017).

MATERIALS AND METHODS

1-Drugs:

Contramal (tramadol HCl) is provided as 100 mg tablets (Grunenthal, Italy). Thyme aqueous extract was made with dry thyme leaves purchased from a local store. Using an electrical chopper, the leaves of the thyme were crushed into a fine powder. The powder was then extracted for 30 minutes in a covered flask with 200 ml of boiling distilled water (DW). The extract was cooled then filtered to eliminate any particle matter. The filtrate was then vacuum-dried. Before delivery, the appropriate dosages were weighed and reconstituted in 5 mL of DW (Swayeh *et al.*, 2014).

II-Experimental Animals:

A total of 48 mature female albino rats and 12 adult male albino rats weighing 180-200 grams were used in this work. The animals were taken from Assiut University's Animal House. They have environmental circumstances. The animals were housed in separate cages in an appropriately ventilated room with an average temperature (22-24 C) and humidity and were given unrestricted access to food and water on a regular 12h light/12h dark cycle (El-Bermawy and Salem, 2015).

III-The Experimental Design:

The pregnancy of rats was confirmed by the presence of a vaginal plug. After that, the pregnant female rats were randomly allocated into three main groups; control, tramadol treated and tramadol + thyme treated (Aboulhoda and Hassan, 2018, Sarhan and Taalab, 2018). Each main group was further subdivided into 3 subgroups as follows:

1-Control Group: The pregnant female rats from day one of pregnancy till the end of weaning have not received any medications for 8 weeks. Their offspring were further subdivided into 3 subgroups: 1- A (Newborn), 1-B (postnatal 10th day), and 1-3 (postnatal 20th day).

2-Tramadol Group: The pregnant female rats were given oral dosages of tramadol HCL (40 mg/kg/day) suspended in tap water through an oro-gastric tube from 1st day of pregnancy till weaning. Their offspring were subdivided into 3 subgroups: 2- A (Newborn), 2-B (postnatal 10th day) and 2-C (postnatal 20th day).

3-Tramadol + Thyme Group: From the 1st day of pregnancy until weaning, pregnant female rats were given tramadol HCL (40 mg/kg/day) and thyme extract (500 mg/kg/day) orally via an oro-gastric tube. Their offspring were subdivided into 3 subgroups: 3- A (Newborn), 3-B (postnatal 10th day) and 3-C (postnatal 20th day).

IV- Histological Study:

The rats' offspring of the nine subgroups (3 newborn groups, 3 groups of each on the 10th and the 20th postnatal days) were anesthetized with ether inhalation and perfused with normal saline. After decapitation, the cerebella were removed cautiously from the rat skull. For the light microscopic study, small pieces from the cerebellum were fixed in Bouin's solution for 3 hours, dehydrated in progressively higher alcohol concentrations, cleaned in xylene, and then imbedded in paraffin wax. Serial paraffin sagittal slices of about 5 µm were done for gallocyanin-chrome alum staining to demonstrate Purkinje cell layer (Bancroft and Gamble, 2008).

For the immunohistochemistry study, specimens were fixed in 10% neutral buffered formalin. Preparation for inducible nitric oxide synthase immunohistochemistry using the labelled streptavidin-biotin immunoperoxidase technique was done. The sections were deparaffinized in xylene rehydrated in EtOH and washed twice with distilled water. PBS was used to wash the samples (pH 7.2). The presence of iNOS in the cytoplasm was determined using an immunoperoxidase stain for iNOS (1:200 dilution). The biotinylated secondary antibody was incubated on the slides for 45 minutes, and then the slides were washed and treated with an avidin-biotinylated peroxidase complex reagent. Hematoxylin was used as a

counterstain on the slides. (Zhang *et al.*, 2008).

Small pieces of the cerebellum, 1x1 mm in size, were fixed in 2.5% buffered glutaraldehyde and subsequently processed to obtain semithin and ultrathin slices for electron microscopic investigation. Staining was done on ultrathin sections (60-80 nm) using lead citrate and uranyl acetate. These were examined by JEOL-JEM-100 SX transmission electron microscope in Electron Microscopy unit, Assuit University, Egypt (Friedrich and Mugnaini, 1981).

V- Morphometric Study:

The number of the Purkinje neurons (PNn) per an area of 12753 μ m² by using x400 magnification was measured. The measurements were performed in 10 fields in each of five different sections taken from five different rats of each group. Leica Qwin 500 (Leica Ltd) image analyzer computer system was used to analyze all the images. Data of the study were presented in the form of figures, tables and histograms (El-Bermawy and Salem, 2015).

Statistical Analysis:

Utilizing statistical software, the mean values of the data received from the image analyzer were examined (SPSS V23, Inc., IL, USA). Quantitative parametric data were compared using the one-way analysis of variance (ANOVA) test, followed by the post-hoc Tukey test, whereas quantitative non-parametric data were compared using the Kruskal-Wallis test, then the Dunn's test. Mean and standard error (SE) were used to depict quantitative parametric data, whereas median and interquartile range (IQR) was used to portray quantitative non-parametric data. P<0.05 was considered statistically significant (Altman, 2005).

RESULTS

Histological Study:

I-Group 1- A (Neonatal control group):

By the Gallocyenin staining (GC), The Purkinje cell layer (PCL) showed to be localized on the outer peripheral region of the internal granular cell layer and composed of primitive two cell layers thick. Each cell layer is composed of a large round-shaped cell with

a prominent centrally located nucleus (Plate I-A). Studying the immunohistochemical-stained (IH) sections showed a negative immunoreaction of the cytoplasm of PCL (Plate I-B). By the electron microscopic examination (EM), Purkinje cell revealed the presence of a large nucleus with euchromatic chromatin and a regular double-folded nuclear membrane. The cell perikaryon contained many rounded mitochondria with prominent cristae, rough endoplasmic reticulum cisternae (rER) and a lot of free ribosomes. Intact cell membrane and excess synaptic vesicles were noted. Multiple synaptic spines were in contact with the glial cell process and the synaptic clefts were observed (Plate I-C).

II- Group 2-A (Neonatal Tramadol treated group):

By GC staining, PCL contained some cells with an irregular outline, darkly stained cytoplasm, and an ill-defined nucleus (Plate II-A). Examination of IH-stained sections showed mild positive immunoreaction of the cytoplasm of some Purkinje cells (Plate II-B). Through EM examination, Purkinje cell had focal clumping of the chromatin and an irregularity of the nuclear membrane. Purkinje cell perikaryon was rarified and contained many large vacuoles. The cytoplasmic organelles were disorganized with the presence of multiple vacuolated mitochondria and dilated rough endoplasmic reticulum cisternae. The cell membrane was interrupted. Its perikaryon contained scanty synaptic vesicles, multivesicular bodies and lipofuscin granules (Plate II -C).

III- Group 3-A (Neonatal Tramadol +Thyme treated group):

By GC staining, PCL was differentiated mostly into two layers (Plate III-A). Sections stained by the IH method showed a negative immunoreaction of the cytoplasm of all Purkinje cells (Plate III- B). EM examination showed that Purkinje cell contained a euchromatic nucleus and an irregular nuclear membrane. Purkinje cell perikaryon contained many mitochondria with nearly normal rER. Many synaptic

vesicles and small spaces were present. The cell membrane was intact with the presence of many synaptic spines (Plate III- C).

IV-Group 1- B (Control group of postnatal 10th day):

By GC- staining, PCL was mostly arranged into one row. Purkinje cells appeared of peculiar large size with a rounded shape and composed of centrally situated nuclei that occupied almost all their cell bodies and thin basophilic cytoplasmic cell coat (Plate IV-A). IH stained sections showed a negative immunoreaction of the cytoplasm of Purkinje cells (Plate IV-B). By EM examination, Purkinje cell revealed a large nucleus with euchromatic chromatin. Purkinje cell nucleus was surrounded by a regular double nuclear membrane. It contained many mitochondria, many rER, free ribosomes and synaptic vesicles. The cell membrane was intact with the presence of some synaptic spines (Plate IV-C).

V-Group 2- B (Tramadol treated group of postnatal 10th day):

By GC - staining, PCL revealed some deformed and shrunken Purkinje cells with ill-definite nuclei. It was separated from the internal granular layer (Plate V-A). IH stained sections showed a strong positive immunoreaction of the cytoplasm of the Purkinje cells (Plate V - B). By EM, Purkinje cell had a nucleus with an irregular double nuclear membrane and rarified vacuolated chromatin. The cell perikaryon contained multiple vacuoles, swollen mitochondria with destroyed cristae, dilated rER, multivesicular bodies and lipofuscin granules. The cell membrane was interrupted and ill-defined (Plate V- C).

VI- Group 3-B (Tramadol +Thyme treated group of postnatal 10th day):

GC- staining sections showed that PCL was differentiated into one row of large rounded cells containing vesicular nuclei. A few shrunken Purkinje cells with ill-defined nuclei were found (Plate VI-A). IH stained sections showed a mild positive immunoreaction of the cytoplasm of some Purkinje cells (Plate VI- B). By EM, Purkinje cell showed a large euchromatic nucleus with

a folded double nuclear membrane. Purkinje cell perikaryon contained many mitochondria of cristae pattern, few dilated rER with loss of the ribosomal granules and nearly normal synaptic vesicles. The cell membrane was clearly apparent with multiple synaptic spines. Well-preserved myelin sheath was present (Plate VI- C).

VII-Group 1- C (Control group of Postnatal 20th day):

GC-stained sections showed that PCL was formed of rounded to flask-shaped cells with well-defined rounded vesicular nuclei. In between Purkinje cells, there were the glial cells. (Plate VII -A). IH stained sections showed a negative immunoreaction of the cytoplasm of the Purkinje cell (Plate VII - B). By EM, the Purkinje cell revealed a large euchromatic nucleus having a prominent nucleolus with a double-folded nuclear membrane. Its perikaryon contained many rounded and elongated mitochondria with cristae patterns, many rER and free ribosomes. The cell membrane could be clearly seen (Plate VII – C).

VIII-Group 2- C (Tramadol treated group of Postnatal 20th day):

By GC, PCL was disorganized. Some Purkinje cells had darkly stained nuclei and were surrounded by per-cellular haloes (Plate VIII –A). IH sections showed a strong positive immunoreaction of the cytoplasm of some Purkinje cells and moderate immune reactivity in others (Plate VIII - B). EM examination showed Purkinje cell with a nucleus having condensed chromatin and surrounded by an irregular and ill-defined nuclear membrane. Its perikaryon contained many large vacuoles, mitochondria with destroyed cristae, swollen vacuolated mitochondria and. The cell membrane was interrupted. Rarefaction of the extracellular matrix was observed (Plate VIII - C).

IX-Group 3- C (Tramadol + Thyme treated group of Postnatal 20th day):

By GC the PCL had mostly intact large rounded vesicular nuclei. Purkinje cells were arranged in one row. A few shrunken Purkinje cells were found (Plate IX -A). IH sections showed a mild positive

immunoreaction of the cytoplasm of a few Purkinje cells (Plate IX - B). EM examinations of Purkinje cells showed a large nucleus having euchromatic chromatin and surrounded by a regular nuclear membrane. Its perikaryon contained few mitochondria with mild degenerative changes. Many of the

rER were preserved and a few ones were slightly dilated. The cell membrane was intact with the presence of many synaptic spines in contact with many glial cell processes. Multiple synaptic clefts could be seen (Plate IX -C).

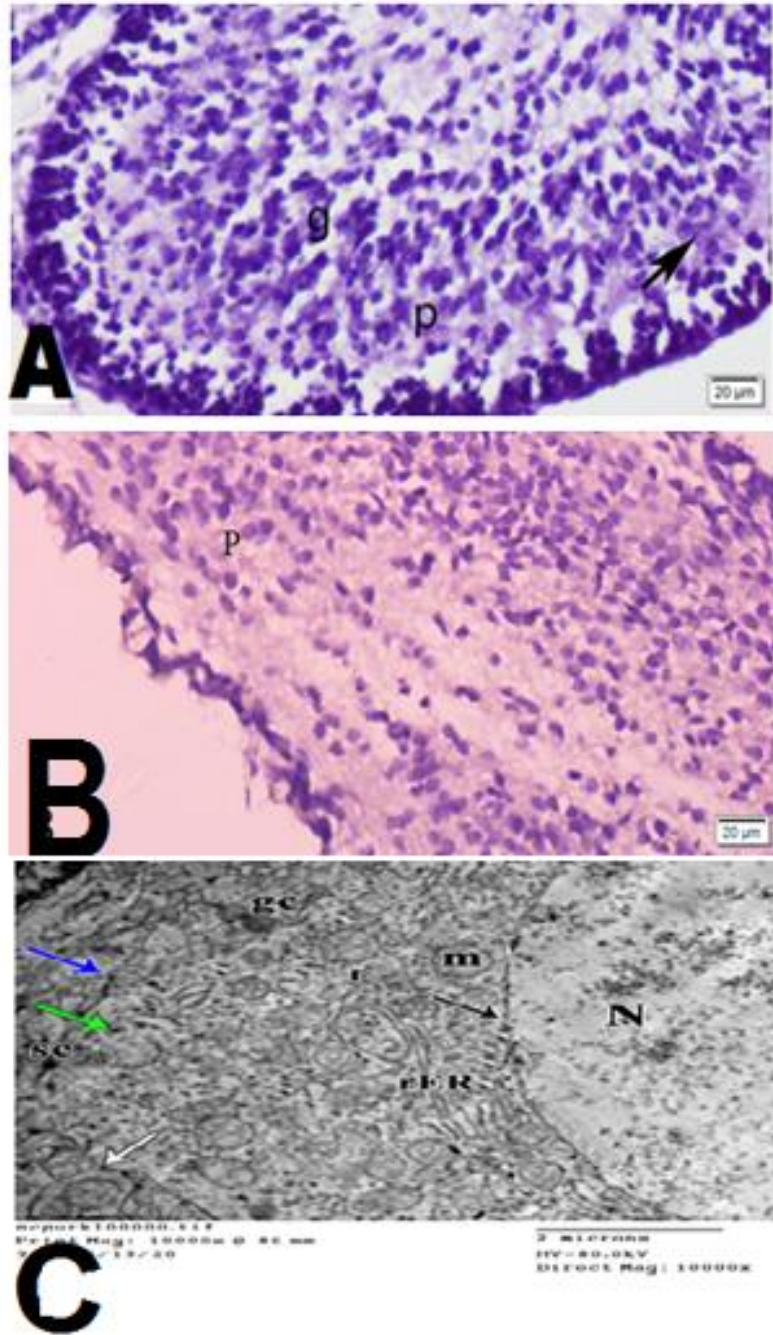


Plate I: The cerebellar cortex of a newborn rat of the control group, (A)- a *gallocyanin chrome-alum-stained sagittal section* ($\times 400$) showing the Purkinje cell layer (p) is localized on the outer peripheral region of the internal granular cell layer (g) and it is composed of primitive two cell-layers thick. Each cell layer is composed of large round-shape cells with prominent centrally located nuclei (black arrow). (B)- An *immunostained for iNOS photomicrograph* ($\times 400$) showing a negative immunoreaction of the cytoplasm of the cells of the Purkinje layer (p). (C)- An *electron micrograph of Purkinje cell* ($\times 10000$) showing part of the nucleus (N) that contains a euchromatic chromatin. It has regular double folded nuclear membrane (black arrow). The perikaryon contains many rounded mitochondria (m), rough endoplasmic reticulum cisternae (rER) with ribosomal granules and free ribosomes (r). An intact cell membrane (white arrow) and synaptic vesicles (green arrow) are noted. Multiple synaptic spines (blue arrow), glial cell processes (gc) and synaptic clefts (sc) are observed.

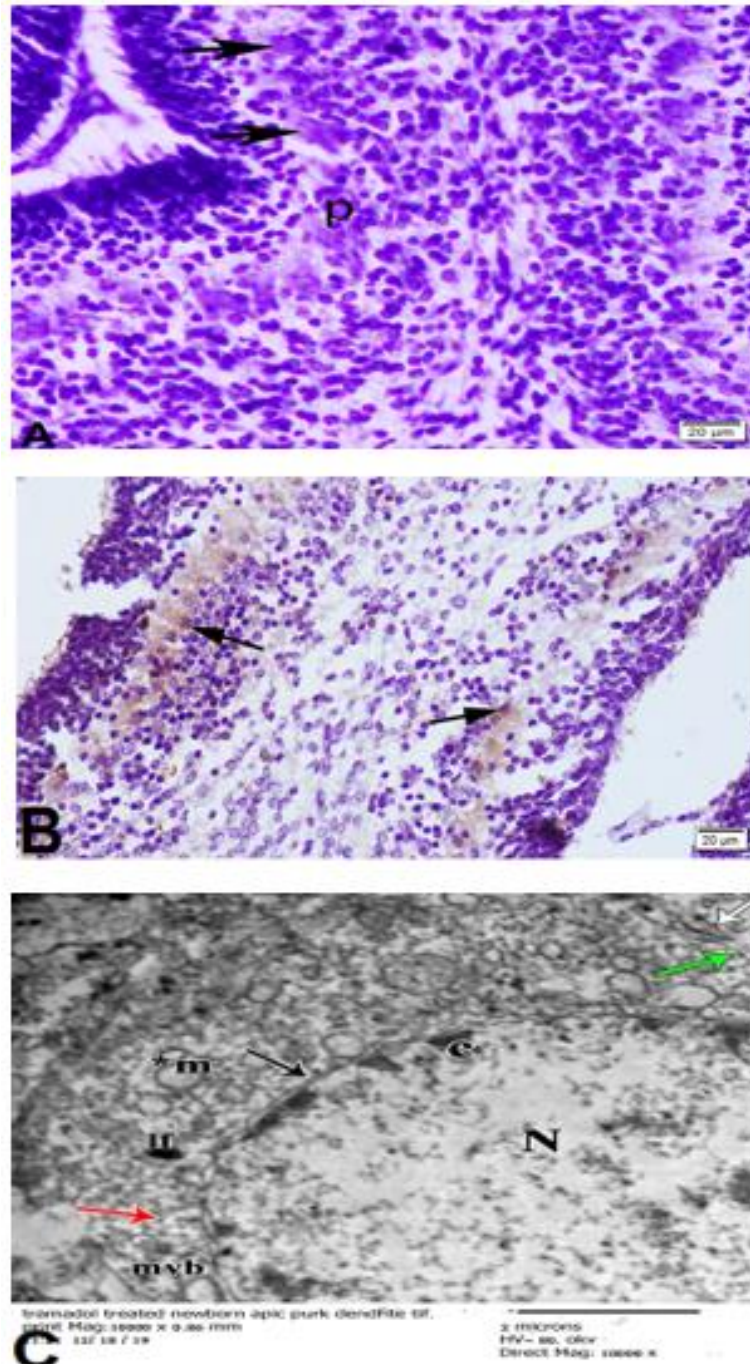


Plate II: The cerebellar cortex of a newborn rat of the tramadol group, (A)- *a gallocyanin chrome-alum-stained sagittal section* ($\times 400$) showing the Purkinje cell layer (p) appears ill differentiated into two layers and some cells have an irregular outline with darkly stained cytoplasm and an ill-defined nucleus (black arrow). (B)- *An immunostained for iNOS photomicrograph* ($\times 400$) showing a mild positive immunoreaction of the cytoplasm of some Purkinje cells (arrow). (C)- *An electron micrograph of Purkinje cell* ($\times 10000$) showing part of the nucleus (N) with multiple focal clumping of the chromatin (c) that become more adherent to the nuclear membrane and an indented nuclear membrane (black arrow). The perikaryon contains many spaced mitochondria (*m) and disorganized destroyed rough endoplasmic reticulum cisternae (red arrow). The cell membrane is interrupted with absence of the synaptic spines (white arrow). Scanty synaptic vesicles (green arrow), multivesicular bodies (mvb) and lipofuscin granules (lf) are noted.

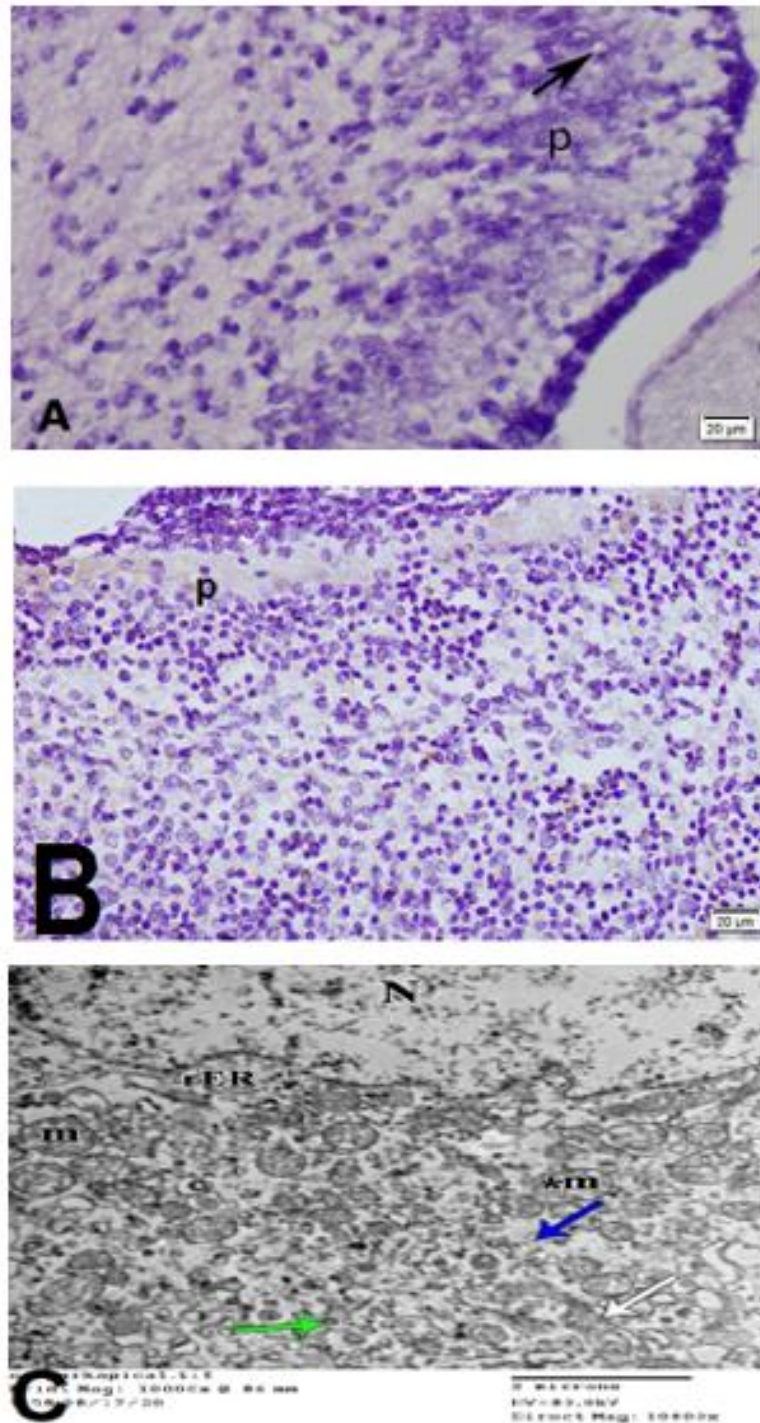


Plate III: The cerebellar cortex of a newborn rat of the tramadol + thyme group, (A)- *gallocyanin chrome-alum-stained sagittal section* ($\times 400$) shows the Purkinje layer (p) is differentiated into two or more layers with few cells contain eccentric pyknotic nuclei (black arrow). (B)- *An immunostained for iNOS photomicrograph* ($\times 400$) showing a negative immunoreaction of the cytoplasm of the cells of the Purkinje layer (p). (C)- *An electron micrograph of Purkinje cell* ($\times 10000$) showing part of the nucleus (N) with an euchromatic chromatin. Purkinje cell perikaryon contains rounded mitochondria (m). A mitochondrion with matrix of focally increased translucence (*m) is observed. An apparent normal shape and organization of the rough endoplasmic reticulum cisternae (rER) and many synaptic vesicles (green arrow) are noted. The cell membrane (white arrow) is intact with the presence of many synaptic spines (blue arrow).

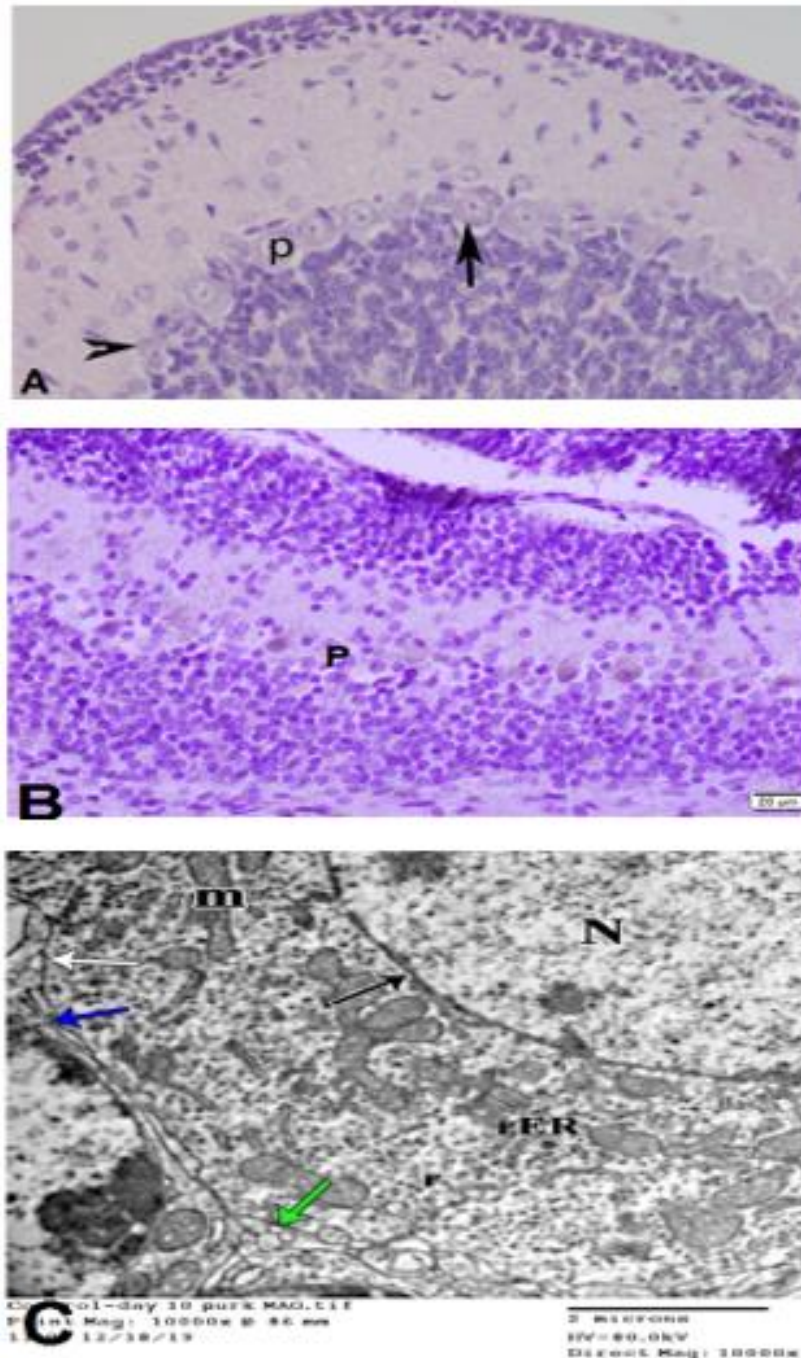


Plate IV: The cerebellar cortex of a 10 days old rat of the control group, (A)- *gallocyanin chrome-alum-stained sagittal section* ($\times 400$) shows Purkinje cell layer (p) is regularly arranged into a single row. Purkinje cell (black arrow) has large size and round shape. It is composed of centrally situated nucleus occupied almost of its cell body and has a thin basophilic cytoplasmic cell coat. There is small round lightly stained glial cells (arrow head) in between Purkinje cells. (B)- *An immunostained for iNOS photomicrograph* ($\times 400$) showing a negative immunoreaction of the cytoplasm of the cells of the Purkinje layer (p). (C)- *An electron micrograph of Purkinje cell* ($\times 10000$) showing part of a nucleus (N) with a euchromatic chromatin. The nucleus is surrounded by a regular double nuclear membrane (black arrow). Purkinje cell perikaryon contains many rounded and elongated mitochondria (m), rough endoplasmic reticulum (rER), and free ribosomes (r). The cell membrane (white arrow) is intact with presence of some synaptic spines (blue arrow). The synaptic vesicles (green arrow) can be noted.

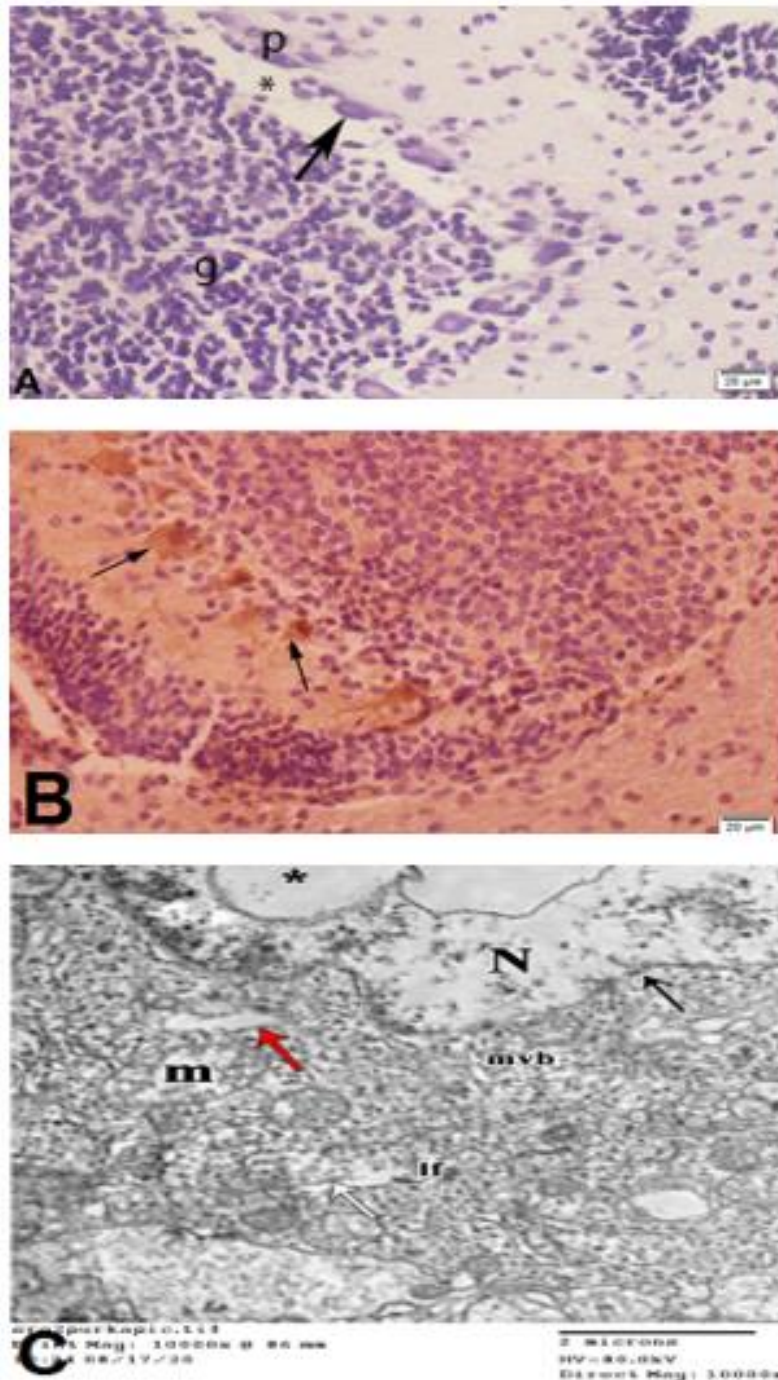


Plate V: The cerebellar cortex of a 10 days old rat of the tramadol group, (A)- *a gallocyanin chrome-alum-stained sagittal section* ($\times 400$) shows Purkinje cell layer (p) containing some deformed and shrunken Purkinje cells with ill-definite nuclei (black arrow). The Purkinje layer is separated (asterisks) from the internal granular layer (g). (B)- *An immunostained for iNOS photomicrograph* ($\times 400$) showing a strong positive immunoreaction of the cytoplasm of many Purkinje cells (black arrow). (C)- *An electron micrograph of Purkinje cell* ($\times 10000$) showing part of the nucleus (N) with irregular double nuclear membrane (black arrow) and a large area of rarefaction (asterisks). The cell perikaryon contains swollen mitochondria of destroyed cristae (m) and dilated rough endoplasmic reticulum cisternae (red arrow) with loss of the ribosomal granules. The cell membrane (white arrow) is interrupted and ill-defined. Multivesicular bodies (m vb) and lipofuscin granules (lf) are present.

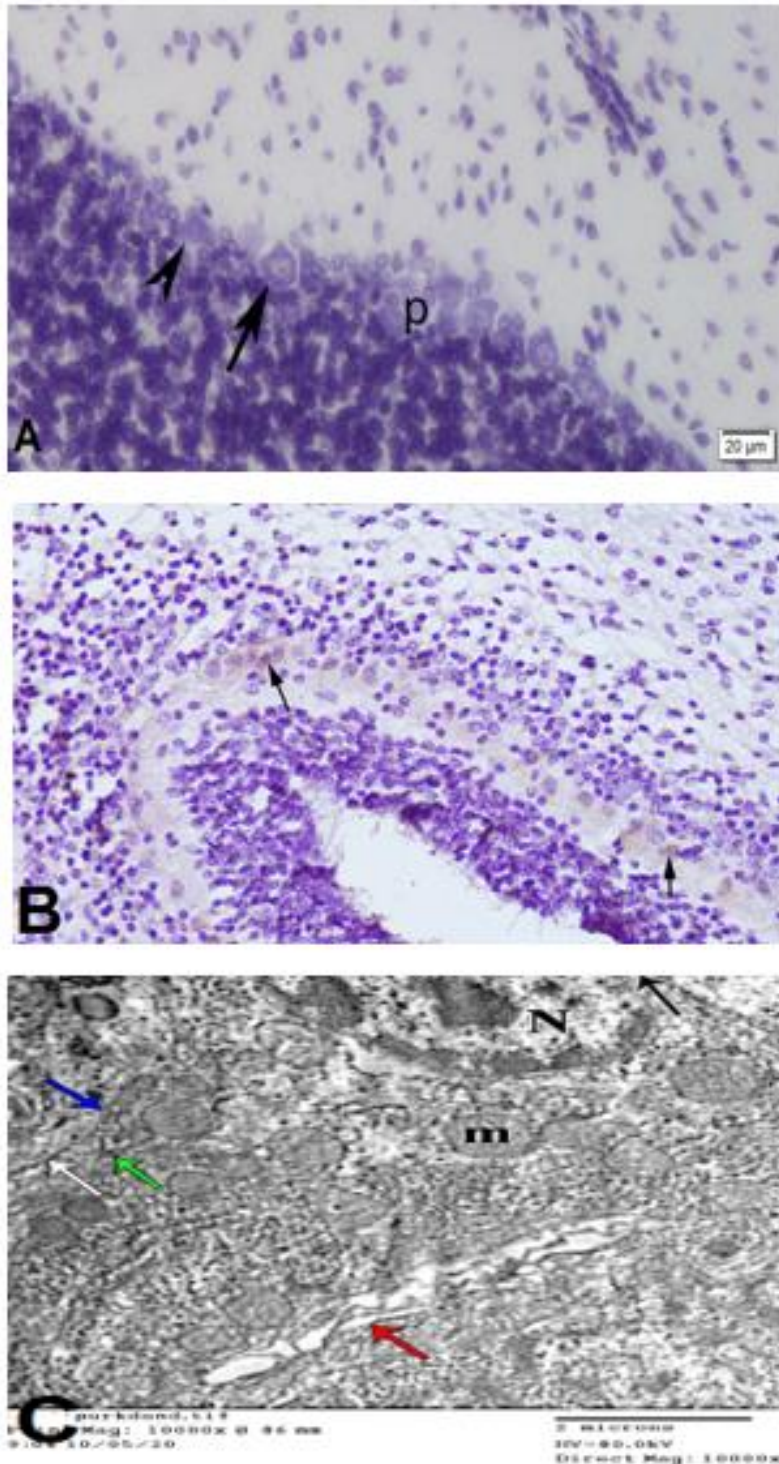


Plate VI: The cerebellar cortex of a 10 days old rat of the tramadol + thyme group, (A)- *a gallocyanin chrome-alum-stained sagittal section* ($\times 400$) shows the Purkinje layer (p) contains mostly normal Purkinje cells with vesicular nuclei (black arrow). Few shrunken Purkinje cells with ill-defined nuclei (arrow head) can be seen in some areas. (B)- *An immunostained for iNOS photomicrograph* ($\times 400$) showing a mild positive immunoreaction of the cytoplasm of some Purkinje cells (black arrow). (C)- *An electron micrograph of Purkinje cell* ($\times 10000$) showing a part of the nucleus (N) with euchromatic chromatin and surrounded by double folded nuclear membrane (black arrow). Intact cristae of the most of the mitochondria (m) and few dilated rough endoplasmic reticulum cisternae (red arrow) are observed. The cell membrane could be seen (white arrow).

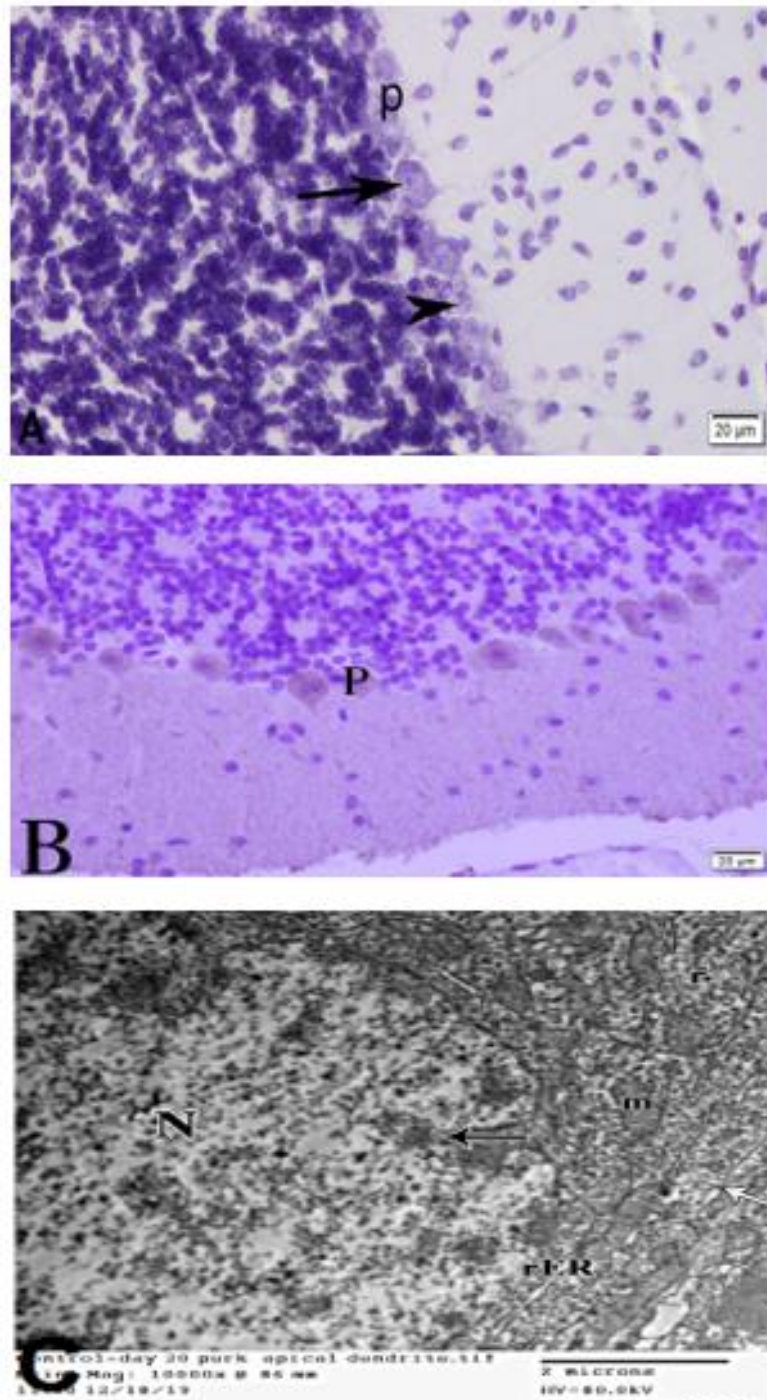


Plate VII: The cerebellar cortex of a 20 days old rat of the control group, (A)- *a gallocyanin chrome-alum-stained sagittal section* ($\times 400$) shows Purkinje cell layer (p) is formed of round to flask shaped cells with round vesicular nuclei (black arrow). In between Purkinje cells, there are the glial cells (arrow head). (B)- *An immunostained for iNOS photomicrograph* ($\times 400$) showing a negative immunoreaction of the cytoplasm of the cells of the Purkinje layer (p). (C)- *An electron micrograph of Purkinje cell* ($\times 10000$) showing part of the nucleus (N) comprises homogeneously scattered euchromatin and small heterochromatin granules. The nucleus is surrounded by a double folded nuclear membrane (black arrow). The perikaryon contains many rounded and elongated mitochondria (m) of cristae pattern, rough endoplasmic reticulum cisternae (rER) and free ribosomes (r). The cell membrane is clearly seen with the presence of the spiny appearance (white arrow).

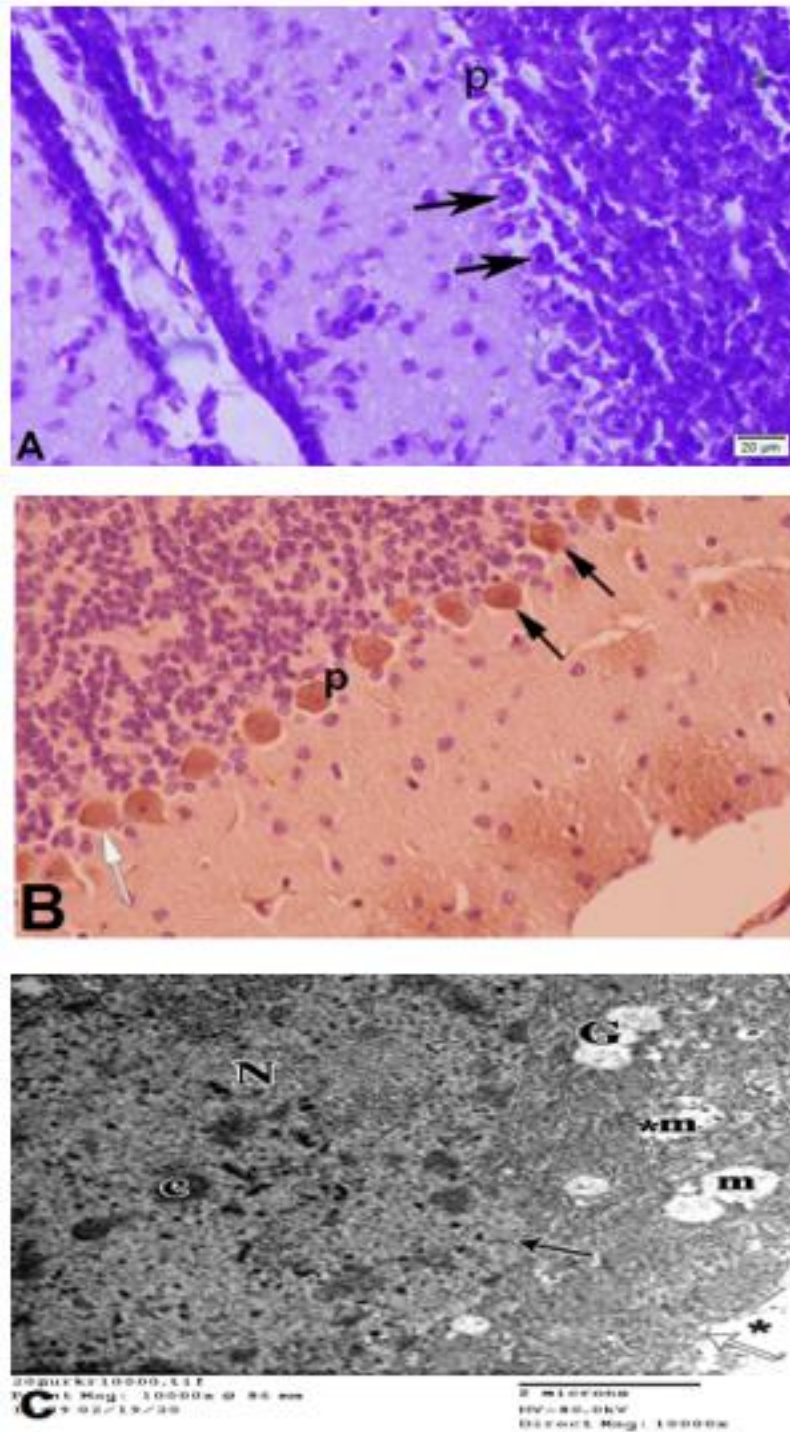


Plate VIII: The cerebellar cortex of a 20 days old rat of the tramadol group, (A)- *a gallocyanin chrome-alum-stained sagittal section* ($\times 400$) shows Purkinje cell layer (p) contains some cells having darkly stained nuclei and surrounded by per cellular haloes (black arrow). (B)- *An immunostained for iNOS photomicrograph* ($\times 400$) showing a moderate positive (white arrow) and a strong positive (black arrow) immunoreaction of the cytoplasm of Purkinje cells. (C)- *An electron micrograph of Purkinje cell* ($\times 10000$) showing part of the nucleus (N) that contains many spots of the condensed chromatin (c) and surrounded by an irregular ill-defined nuclear membrane (black arrow). The cell perikaryon contains many swollen vacuolated mitochondria (m), mitochondria with destroyed cristae (*m) and dilated cisternae of Golgi apparatus (G). The cell membrane is interrupted (white arrow) with absence of the spiny appearance. Extra cellular rarefaction is noted (asterisks).

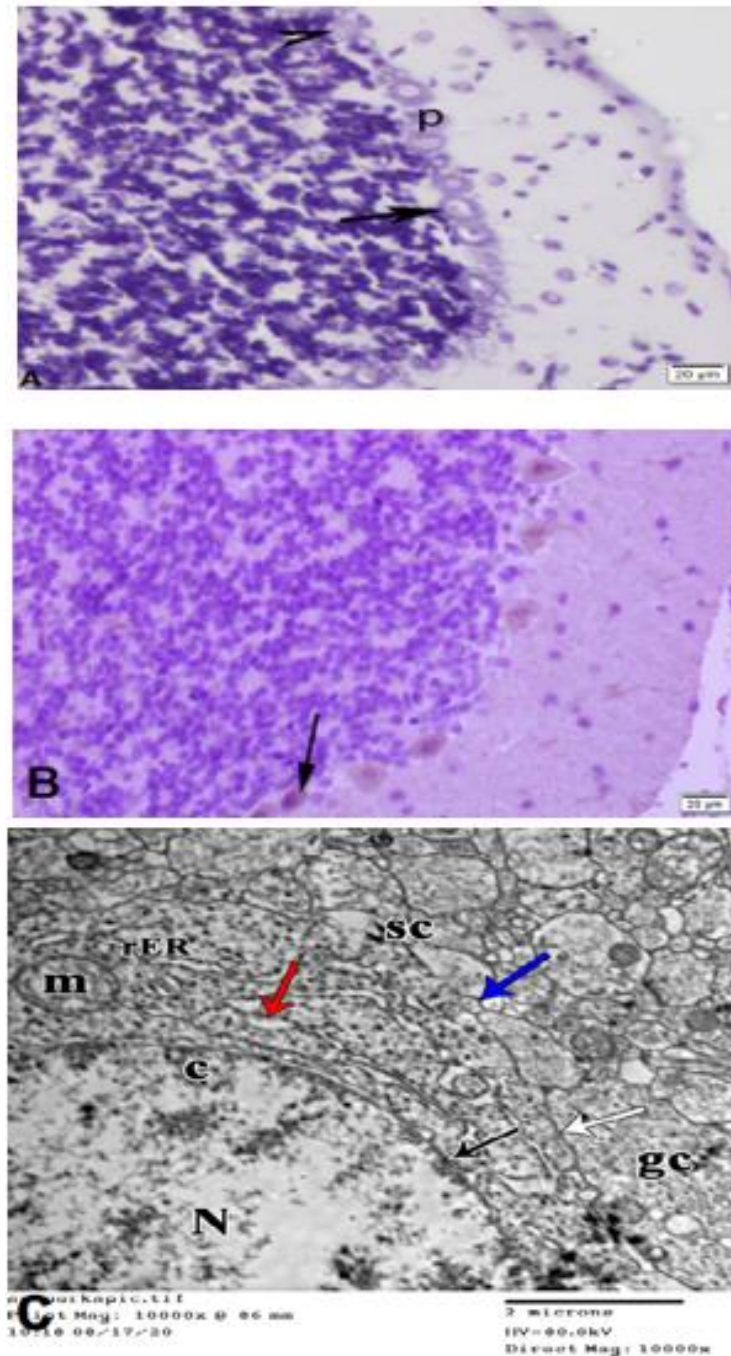


Plate IX: The cerebellar cortex of a 20 days old rat of the tramadol + thyme group, (A)- a gallocyanin chrome-alum-stained sagittal section ($\times 400$) shows the Purkinje layer (p) contains relatively intact Purkinje cells with vesicular nuclei (black arrow). Few withered Purkinje cells (arrow head) are found in some areas. (B)- An immunostained for iNOS photomicrograph ($\times 400$) showing a mild positive immunoreaction of the cytoplasm of few Purkinje cells (black arrow). (C)- An electron micrograph of Purkinje cell ($\times 10000$) showing part of the nucleus (N) with a euchromatin (c) and surrounded by a regular double nuclear membrane (black arrow). Mitochondria with minimal degenerative changes (m) are present. Most of cisternae of the rough endoplasmic reticulum (rER) are preserved with presence of ribosomal granules except few ones are slightly dilated (red arrow). The cell membrane (white arrow) is intact with presence of many synaptic spines (blue arrow) in contact with many glial cell processes (gc). Multiple synaptic clefts (sc) are observed.

Morphometric Results:

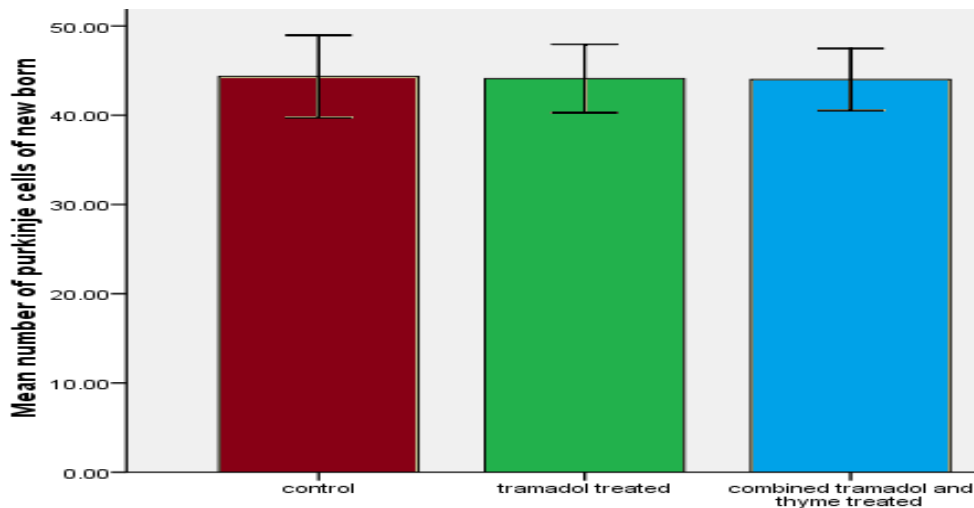
ANOVA analyses of PNn in the neonatal age revealed insignificant statistical differences among the three groups (p value > 0.05). This difference could indicate that prenatal administration of tramadol has no effect on the PNn of the cerebellar cortical development of the newborn pups (**Table 1 & Histogram 1**).

In studying the mean PNn of the 10th postnatal day, ANOVA analysis found a significant difference between the three groups (p value < 0.05). This difference also indicated that administration of tramadol decreased the PLT as a sign of degeneration and this effect is partially improved by the combined use of thyme as a sign of regeneration (**Table 2 & Histogram 2**).

Table 1: Comparison among the mean PNn of newborn in different groups.

Groups	Groups	Mean \pm SE
G1	G I	44.33 \pm 2.01
G2	G II	44.11 \pm 1.66
G3	GIII	44.20 \pm 1.51

G I (control group), G II (tramadol treated), GIII (tramadol + thyme treated), Data are means \pm SE from five to ten rats/group.

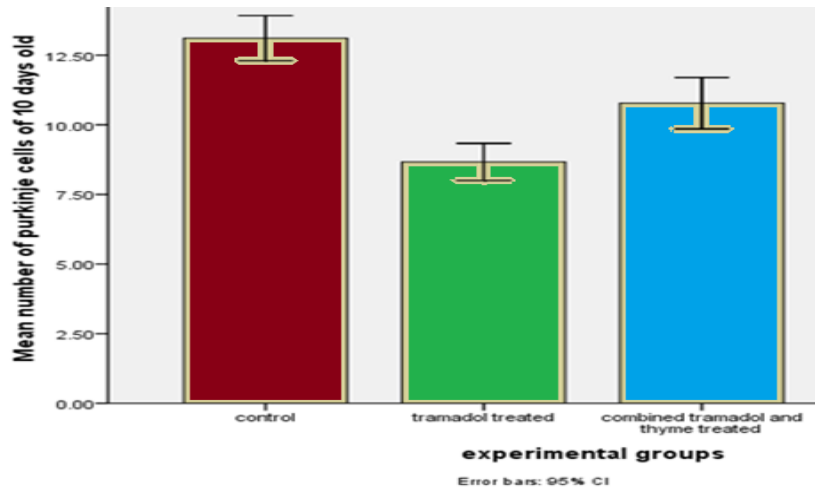


Histogram 1: The relations among the mean PNn of newborn age in the different experimental groups.

Table 2: Comparison among the mean PNn in postnatal 10th day in the different experimental groups.

Groups	Mean \pm SE
G1	13.11 \pm 0.35(#\$)
G2	8.67 \pm 0.29(*\$)
G3	10.78 \pm 0.40(#*)

G I (control group), G II (tramadol treated), GIII (tramadol + thyme treated), Data are means \pm SE from five to ten rats/group. * significantly different ($p < 0.05$) from group I. # significantly different ($p < 0.05$) from group II. \$ significantly different ($p < 0.05$) from group III.



Histogram 2: The relations among the mean PNn of postnatal 10th day in the different experimental groups.

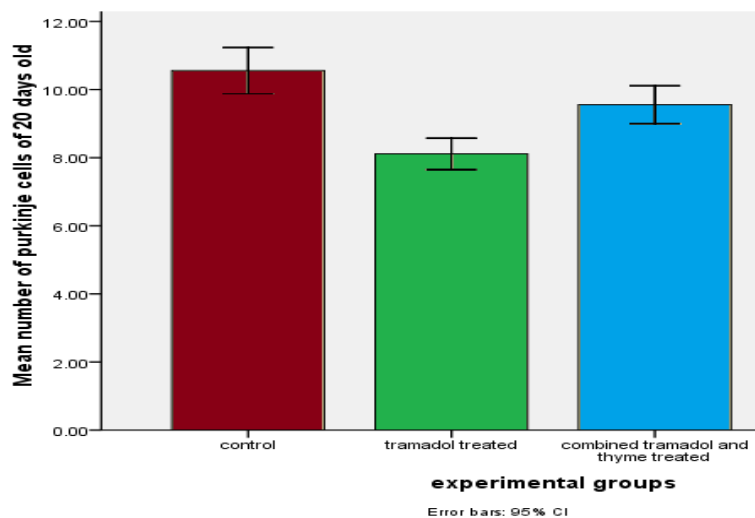
In the postnatal 20th day old, there was a significant statistical difference among the three groups (p value < 0.05). This again denoted that administration of tramadol decreased the MLT, PLT and GLT of the

cerebellar cortex of the adult rats as a sign of degeneration and this effect was partially by the combined use of thyme as a sign of regeneration (**Table 3 & Histogram 3**).

Table 3: Comparison among the mean PNn in postnatal 20th day groups.

Groups	Mean ± SE
G1	10.56 ± 0.29(#\$)
G2	8.11 ± 0.20(*\$)
G3	9.56 ± 0.24(#*)

G1 (control group), G2 (tramadol treated), G3 (tramadol + thyme treated), Data are means ± SE from five to ten rats/group. * significantly different (p < 0.05) from group I. # significantly different (p < 0.05) from group II. \$ significantly different (p < 0.05) from group III.



Histogram 3: The relations among the mean PNn of postnatal 20th day in the experimental groups.

DISCUSSION

The current study aimed to evaluate the histological, morphometric and immunohistochemical postnatal changes in the Purkinje cell layer of the cerebellar cortex of albino under the effect of maternal tramadol administration during pregnancy and lactation as well as the possible protective effect of the concomitant use of thyme extract. In the present study, Purkinje cells were used as a model of the study because of their fundamental role in controlling motor movement and their dysfunction and loss are responsible for cerebellar ataxia (Yang *et al.*, 2022).

In the control group of the present study, LM examination of the Purkinje cell layer of the newborn rat revealed that this layer is localized on the outer peripheral region of the internal granular cell layer and composed of primitive two cell layers thick. Each cell layer is composed of a large round-shaped cell with prominent centrally located nucleoli. In harmony with our result, a previous study supports our results (El-Sayyad *et al.*, 2015). On the postnatal 10th day, Purkinje cells showed an obvious increase in the size of their cell bodies. They appeared of peculiar large size with a rounded shape and composed of centrally situated nuclei that occupied most of the cell bodies and a thick basophilic cytoplasmic cell coat. These observations were in a harmony with the studies of Allam *et al.*, (2011), Abdel-Hafez and Mohamed, (2013). On a postnatal day 20, Purkinje cells attained much more, and the differentiation was regularly arranged at the periphery of the internal granular layer. These cells were characterized by their huge large cell bodies with prominent centrally located nuclei and vesicular nucleoli. These results were in accordance with the study of Sotelo and Rossi, (2021) who reported similar findings. By EM examination, Purkinje cells of the three main studied age groups of the control group showed that they had a large nucleus containing prominent nucleolus. The nucleus was surrounded by a double-folded nuclear membrane. Its perikaryon contained

many rounded and elongated mitochondria with cristae patterns, many rER with ribosomal granules and a lot of free ribosomes. These results were in accordance with the studies of Shona *et al.*, (2018) , Badawy and Mohammed, (2021).

In the tramadol group of the current study, LM examination of the Purkinje cell layer of the newborn rats revealed degenerative changes as evidenced by the presence of some Purkinje cells with darkly stained or pyknotic nuclei. This may be explained on the basis that most Purkinje cells settle in the developing cerebellum after birth to the first month as reported by Altman, (1997). Furthermore, numerous studies revealed that tramadol use in increasing doses led to neuron degeneration in the rat brain, which may be a factor in brain impairment (Barsotti, Mycyk and Reyes, 2003 , Atici *et al.*, 2004). In harmony with these results, Elfeky and Mohamed, (2017) noticed that the histopathologic alterations in brain tissues appear to be the outcome of neuronal exhaustion brought on by sustained increased activity in response to ongoing tramadol treatment. The observed pericellular spaces in the Purkinje cell layer in the current study might be due to the shrinkage of cells with the withdrawal of their processes secondary to cytoskeleton affection. Previous research indicated that long-term opioid usage led to cell apoptosis with cytoplasmic contraction, a decrease in cell volume, chromatin condensation, and neuronal injury through affecting their cytoskeleton (Ragab and Mohamed, 2017). Axonal degeneration of Purkinje cells causing by damage of the vital DNA, lipids and protein macromolecules of the cells could be another explanation (Shona *et al.*, 2018).

By EM examination of the tramadol group, the degenerative changes of Purkinje cells appeared in all different studied ages and increased from the newborn to the 20th postnatal day. The degenerative changes of Purkinje cells were in form of the irregular nuclear membrane, focal clumping of the chromatin, rarefaction of the perikaryon,

disorganization of the cytoplasmic organelles with the presence of multiple vacuolated or destroyed mitochondria, lipofuscin granules, scanty synaptic vesicles and dilated rER with the absence of their ribosomal granules and interruption of the cell membrane with less developed synaptic spines. In harmony with these findings, Mao *et al.*, (2002), Farber and Olney, (2003) stated the cerebellar-damaging effects of opioids including tramadol were reduced Purkinje cell proliferation, cell differentiation and increased Purkinje cell death.

Furthermore, El-Bermawy and Salem, (2015), Sarhan and Taalab, (2018) indicated that the tramadol group's cerebral and cerebellar cortex displayed striking changes in the ultrastructure of Purkinje cells, becoming degraded, dense, and shrunken cells with signs of death like chromatin margination, corrugated nuclear membranes, and aberrant organelles.

In this study, the observed mitochondrial alterations in Purkinje cells might be related to oxidative and endoplasmic reticulum stress (Xia *et al.*, 2020). In endoplasmic reticulum-stressed cells, increased Ca²⁺ release opened the mitochondrial permeability transition pore with loss of cytochrome C. This in turn activated nitric oxide synthetase leading to ROS production. ROS caused more Ca²⁺ release and created a vicious cycle that induces mitochondrial dysfunction and induced apoptosis (Brand, 2010, Cao and Kaufman, 2014).

The Dilated rER might be also due to tramadol-induced lipid peroxidation which could predispose it to oxidative stress during increased load of protein folding (Santos *et al.*, 2009). The degenerative spaces/rarefaction of Purkinje cell perikaryon could be attributed to the damaged cell organoid from exposure to free radicals (Brown *et al.*, 2004, Zarnescu *et al.*, 2008). The little number of synaptic vesicles and degeneration of synaptic spines were caused by the neurotransmitter system being disrupted after tramadol uptake (Baghishani *et al.*, 2018).

In the present study, the tramadol group showed positive cytoplasmic immunoreaction of Purkinje cells that increased from the newborn to the 20th postnatal day. This result was supporting the findings of the study of Abdelaleem *et al.*, (2017) who stated a positive iNOS and Caspase-8 expression in the cytoplasm of cells of all zones of the adrenal cortex of rats in the tramadol-treated group.

The positive immunoreaction in this study may also be explained on basis that tramadol might cause vascular endothelial damage which in turn induced vascular congestion, leading to the release of iNOS which increased NO concentration caused nitration of the cell protein leading to brain inflammation and neurodegeneration (Heneka and Feinstein, 2001).

In the tramadol + thyme group, examination of light and electron microscopic of the Purkinje cell layer in all studied age groups revealed an improvement in the degenerative changes in the case of uptaking thyme with tramadol. These improvements of the degenerative changes increased from the newborn to the 20th postnatal day. This indicates that thyme has ameliorative effects. One of the recent explanation is that thyme extract significantly inhibited the production of iNOS mRNA expression and subsequently decreased cellular injury (Wautier and Wautier, 2022). Also, improvements in the immunohistochemical findings as evidenced by negative cytoplasmic immunoreaction of Purkinje cells of all the different studied age groups were recorded in the tramadol + thyme group. On the same basis, this might be referred to as the protective of thyme extract (Swayeh *et al.*, 2014). These findings confirm the results of Mohammadnejad and Soltaninejad, (2022).

The morphometric results of our study revealed that there was a significant statistical difference at 10th and 20th postnatal age whereas no recorded significant statistical difference at newborn age among the experimental groups. One of the explanations of such results could be attributed to a report of El-Bermawy and Salem, (2015) who

declared that the tramadol neurotoxic effect on the cerebellar structure is an ascending one according to the dose and time of exposure. In this regard, Fonnum and Lock, (2004), said that the Purkinje neurons in rat embryos originate between days 14 and 15 of gestation; at birth, they form a layer that is six cells thick, which by postnatal days 3 to 4 reduces to a single layer., so for a neurotoxic effect to start to appear needs more time. They also noted that administering methyl azoxy methanol to newborn rats within 24 hours of birth causes a significant decrease in cerebellar granule cell numbers, but not Purkinje cell numbers. In harmony with the present study, Sarhan and Taalab, (2018) reported a neuroprotective effect of thyme against the tramadol neurotoxic effect.

CONCLUSION

Maternal tramadol intake during pregnancy and lactation exerted a neurotoxic effect on the postnatal development of the Purkinje cell layer of the cerebellar cortex. Thyme extract can improve these tramadol effects but not repair them completely so this may be helpful as adjuvant administration in the management of tramadol neuronal damage if the use of tramadol is necessary.

Ethical Approval: The experiments were approved by the Institutional Board Review and Ethics Committee of the Faculty of Medicine, Assiut University.

REFERENCES

- Abdel-Hafez, A.M.M. and Mohamed, N.A. (2013): Effect of selenium in ameliorating the effect of induced perinatal hypothyroidism on postnatal rat cerebellar cortex development: a histological and immunohistochemical study. *Egyptian Journal of Histology*, 36(3), pp. 660–680.
- Abdelaleem, S.A. *et al.* (2017): Tramadol induced adrenal insufficiency: histological, immunohistochemical, ultrastructural, and biochemical genetic experimental study. *Journal of toxicology*. <https://doi.org/10.1155/2017/9815853>
- Aboulhoda, B.E. and Hassan, S.S. (2018): Effect of prenatal tramadol on postnatal cerebellar development: Role of oxidative stress. *Journal of Chemical Neuroanatomy*, 94, pp. 102–118. Available at: <https://doi.org/10.1016/J.JCHEMNEU>.
- Allam, A. *et al.* (2011): Prenatal and perinatal acrylamide disrupts the development of cerebellum in rat: biochemical and morphological studies. *Toxicology and Industrial Health*, 27(4), pp. 291–306.
- Altman, G.D. (2005): Comparing groups: three or more independent groups of observations in practical statistics for medical research. *Chapman and Hall* [Preprint].
- Altman, J. (1997): Development of the cerebellar system. *Relation to its Evolution, Structure, and Functions*. [Preprint].
- Atici, S. *et al.* (2004): Opioid neurotoxicity: comparison of morphine and tramadol in an experimental rat model. *International journal of neuroscience*, 114(8), pp. 1001–1011.
- Badawy Khair, N.S. and Mohammed, S.A. (2021): A comparative study on the protective role of Silymarin and Coenzyme-Q10 on the cerebellar cortex of experimentally induced atherosclerosis in adult male albino rats: a histological, immunohistochemical and biochemical study. *Egyptian Journal of Histology*, 44(2), pp. 322–338.
- Baghishani, F. *et al.* (2018): The effects of tramadol administration on hippocampal cell apoptosis, learning and memory in adult rats and neuroprotective effects of crocin. *Metabolic brain disease*, 33(3), pp. 907–916.
- Bancroft, J.D. and Gamble, M. (2008): *Theory and practice of histological techniques*. Elsevier health sciences.
- Barsotti, C.E., Mycyk, M.B. and Reyes, J. (2003): Withdrawal syndrome from tramadol hydrochloride. *The*

- American journal of emergency medicine*, 21(1), pp. 87–88.
- Blanco, S. *et al.* (2010): Study of the nitric oxide system in the rat cerebellum during aging. *BMC neuroscience*, 11(1), pp. 1–14.
- Boonyarattanasoonthorn, T., Khemawoot, P. and Kijawornrat, A. (2021): Comparing Potential Drug–Drug Interactions in Companion Animal Medications Using Two Electronic Databases. *Veterinary sciences*, 8(4), p. 60.
- Brand, M.D. (2010): The sites and topology of mitochondrial superoxide production. *Experimental gerontology*, 45(7–8), pp. 466–472.
- Brown, D.M. *et al.* (2004): Calcium and ROS-mediated activation of transcription factors and TNF- α cytokine gene expression in macrophages exposed to ultrafine particles. *American Journal of Physiology-Lung Cellular and Molecular Physiology*, 286(2), pp. L344–L353.
- Cao, S.S. and Kaufman, R.J. (2014): Endoplasmic reticulum stress and oxidative stress in cell fate decision and human disease. *Antioxidants & redox signaling*, 21(3), pp. 396–413.
- Cicero, T.J. *et al.* (2005): Rates of abuse of tramadol remain unchanged with the introduction of new branded and generic products: results of an abuse monitoring system, 1994–2004. *Pharmacoepidemiology and Drug Safety*, 14(12), pp. 851–859. Available at: <https://doi.org/https://doi.org/10.1002/pds.1113>.
- Dean, L. and Kane, M. (2021): Tramadol therapy and CYP2D6 genotype. *Medical Genetics Summaries [Internet]* [Preprint]. <https://www.ncbi.nlm.nih.gov/books/NBK315950>
- El-Bermawy, M.I. and Salem, M.F. (2015): Histological changes of the albino rat cerebellar cortex under the effect of different doses of tramadol administration. *The Egyptian Journal of Histology*, 38(1), pp. 143–155.
- El-Newary, S.A., Shaffie, N.M. and Omer, E.A. (2017): The protection of Thymus vulgaris leaves alcoholic extract against hepatotoxicity of alcohol in rats. *Asian Pacific journal of tropical medicine*, 10(4), pp. 361–371.
- El-Sayyad, H.I. *et al.* (2015): Impairment of cerebellar cortex and gastrocnemius muscle development of postnatal young of albino rats maternally treated with acrylamide or supplemented food containing fried potatoess chips. *the egyptian journal of experimental biology (Zoology)*, 3, p. 283.
- Elfeky, A. and Mohamed, A. (2017): Effects of Tramadol Addiction on Brain of Adult Male Albino Rats and Role of lofexidine during Withdrawal Period: A Biochemical, Histopathological and Immunohistochemical Study. *Ain Shams Journal of Forensic Medicine and Clinical Toxicology*, 28(1), pp. 119–132.
- Farber, N.B. and Olney, J.W. (2003): Drugs of abuse that cause developing neurons to commit suicide. *Developmental Brain Research*, 147(1), pp. 37–45. Available at: <https://doi.org/https://doi.org/10.1016/j.devbrainres.2003.09.009>.
- Farhan, T.M., Kammona, H.R. and Mubarak, H.J. (2017): The evaluation of histological changes and imunohistochemical expression of amyloid precursor protein in cerebral and cerebellar cortices in newborn mice after prenatal exposure to tramadol. *World Journal of Pharmaceutical Research*, 6(14), pp. 28-43
- Feng, T. *et al.* (2022): TMEM106B deficiency impairs cerebellar myelination and synaptic integrity with Purkinje cell loss. *Acta neuropathologica*

- communications*, 10(1), pp. 1–17.
- Fonnum, F. and Lock, E.A. (2004): The contributions of excitotoxicity, glutathione depletion and DNA repair in chemically induced injury to neurones: exemplified with toxic effects on cerebellar granule cells. *Journal of neurochemistry*, 88(3), pp. 513–531.
- Friedrich, V.L.J. and Mugnaini, E. (1981): Preparation of neural tissues for electron microscopy. in *Neuroanatomical tract-tracing methods*. Plenum Press, New York, pp. 345–375.
- Heneka, M.T. and Feinstein, D.L. (2001): Expression and function of inducible nitric oxide synthase in neurons. *Journal of neuroimmunology*, 114(1–2), pp. 8–18.
- Jerjir, A. *et al.* (2022): Detoxification of Neuromodulation-Eligible Patients by a Standardized Protocol: A Retrospective Pilot Study. *Neuromodulation: Technology at the Neural Interface*, 25(1), pp. 114–120.
- Kabel, J.S. and van Puijenbroek, E.P. (2005): Side effects of tramadol: 12 years of experience in the Netherlands. *Nederlands tijdschrift voor geneeskunde*, 149(14), pp. 754–757. Available at: <http://europepmc.org/abstract/MED/15835626>.
- Khatmi, A. *et al.* (2022): Combined molecular, structural and memory data unravel the destructive effect of tramadol on hippocampus. *Neuroscience Letters*, 771, p. 136418.
- Kuete, V. (2017): *Medicinal spices and vegetables from Africa: therapeutic potential against metabolic, inflammatory, infectious and systemic diseases*. Academic Press, pp. 182–192.
- Mao, J. *et al.* (2002): Neuronal apoptosis associated with morphine tolerance: evidence for an opioid-induced neurotoxic mechanism. *Journal of Neuroscience*, 22(17), pp. 7650–7661.
- Mohamed, T.M., Ghaffar, H.M.A. and El Husseiny, R.M.R. (2015): Effects of tramadol, clonazepam, and their combination on brain mitochondrial complexes. *Toxicology and industrial health*, 31(12), pp. 1325–1333.
- Mohammadnejad, L. and Soltaninejad, K. (2022): Tramadol-Induced Organ Toxicity via Oxidative Stress: A Review Study. *International Journal of Medical Toxicology and Forensic Medicine*, 12(1), p. 35430.
- Paul, M.S. and Limaiem, F. (2021): Histology, Purkinje Cells. in *StatPearls [Internet]*. StatPearls Publishing. <https://pubmed.ncbi.nlm.nih.gov/31424738>.
- Ragab, I.K. and Mohamed, H.Z.E. (2017): Histological changes of the adult albino rats entorhinal cortex under the effect of tramadol administration: Histological and morphometric study. *Alexandria journal of medicine*, 53(2), pp. 123–133.
- Ray, A., Arya, S. and Gupta, R. (2022): Tapentadol-Induced Seizure in a Patient With Opioid Dependence. *The Primary Care Companion for CNS Disorders*, 24(3), p. 41256.
- Santos, C.X.C. *et al.* (2009): Mechanisms and implications of reactive oxygen species generation during the unfolded protein response: roles of endoplasmic reticulum oxidoreductases, mitochondrial electron transport, and NADPH oxidase. *Antioxidants & redox signaling*, 11(10), pp. 2409–2427.
- Sarhan, N.R. and Taalab, Y.M. (2018): Oxidative stress/PERK/apoptotic pathways interaction contribute to tramadol neurotoxicity in rat cerebral and cerebellar cortex and thyme

- enhances the antioxidant defense system: histological, immunohistochemical and ultrastructural study. *International Journal*, 4(6), p. 124.
- Setorki, M. and Mirzapoor, S. (2017): Evaluation of Thymus vulgaris Extract on Hippocampal Injury Induced by Transient Global Cerebral Ischemia and Reperfusion in Rat. *Zahedan Journal of Research in Medical Sciences*, 19(5), pp.103-109. doi: 10.5812/zjrm.s.9216.
- Shona, S.I. *et al.* (2018): Effect of valproic acid administration during pregnancy on postnatal development of cerebellar cortex and the possible protective role of folic acid. *Folia morphologica*, 77(2), pp. 201–209.
- Sotelo, C. and Rossi, F. (2021): Purkinje cell migration and differentiation. in *Handbook of the cerebellum and cerebellar disorders*. Springer, pp. 173–205.
- Subedi, M. *et al.* (2019): An overview of tramadol and its usage in pain management and future perspective. *Biomedicine & Pharmacotherapy*, 111, pp. 443–451.
- Swayeh, N.H. *et al.* (2014): The protective effects of Thymus Vulgaris aqueous extract against Methotrexate-induced hepatic toxicity in rabbits. *Int J Pharm Sci Rev Res*, 29, pp. 187–193.
- Wautier, J.-L. and Wautier, M.-P. (2022): Vascular Permeability in Diseases, *International Journal of Molecular Sciences*, 23(7), p. 3645.
- Xia, W. *et al.* (2020): Toxicology of tramadol following chronic exposure based on metabolomics of the cerebrum in mice. *Scientific reports*, 10(1), pp. 1–11.
- Yang, Y. *et al.* (2022): Loss of Wt1p results in cerebellar ataxia and degeneration of Purkinje cells. *Journal of Genetics and Genomics* [Preprint]. <https://doi.org/10.1016/j.jgg.2022.03.001>
- Zarnescu, O. *et al.* (2008): Immunohistochemical localization of caspase-3, caspase-9 and Bax in U87 glioblastoma xenografts. *Journal of molecular histology*, 39(6), pp. 561–569.
- Zhang, J. *et al.* (2008): Immunolocalization of Kim-1, RPA-1, and RPA-2 in kidney of gentamicin-, mercury-, or chromium-treated rats: relationship to renal distributions of iNOS and nitrotyrosine. *Toxicologic pathology*, 36(3), pp. 397–409.